Genetic tool development in marine protists:

Emerging model organisms for experimental cell biology

Drahomíra Faktorová[1,#,*], R. Ellen R. Nisbet[2,#], José A. Fernández Robledo[3,#], Elena Casacuberta[4,#], Lisa Sudek[5,#], Andrew E. Allen[6,7], Manuel Ares Jr.[8], Cristina Aresté[4], Cecilia Balestreri[9], Adrian C. Barbrook[2], Patrick Beardslee[10], Sara Bender[11], David S. Booth[12], François-Yves Bouget[13], Chris Bowler[14], Susana A. Breglia[15], Anita Broellochs[12], Colin Brownlee[9], Gertraud Burger[16], Heriberto Cerutti[10], Rachele Cesaroni[17], Miguel A. Chiurillo[18], Thomas Clemente[10], Duncan B. Coles[3], Jackie L. Collier[19], Liz Cooney[20], Kathryn Coyne[21], Roberto Docampo[18], Christopher L. Dupont[7], Virginia Edgcomb[22], Elin Einarsson[2], Pía A. Elustondo[15,$], Fernan Federici[23], Veronica Freire-Beneitez[24,25], Nastasia J. Freyria[3], Kodai Fukuda[26], Paulo A. García[27], Peter R. Girguis[28], Fatma Gomaa[28], Sebastian Gornik[29], Jian Guo[5,8], Vladimír Hampl[30], Yutaka Hanawa[31], Esteban R. Haro-Contreras[15], Elisabeth Hehenberger[20], Andrea Highfield[9], Yoshihisa Hirakawa[31], Amanda Hopes[32], Christopher J. Howe[2], Ian Hu[2], Jorge Ibañez[23], Nicholas A.T. Irwin[20], Yuu Ishii[33], Natalia Ewa Janowicz[30], Adam C. Jones[11], Ambar Kachale[1], Konomi Fujimura-Kamada[34], Binnypreet Kaur[1], Jonathan Z. Kaye[11], Eleanna Kazana[24,25], Patrick J. Keeling[20], Nicole King[12], Lawrence A. Klobutcher[35], Noelia Lander[18], Imen Lassadi[2], Zhuhong Li[18], Senjie Lin[35], Jean-Claude Lozano[13], Fulei Luan[10], Shinichiro Maruyama[33], Tamara Matute[23], Cristina Miceli[36], Jun Minagawa[34,37], Mark Moosburner[6,7], Sebastián R. Najle[4,38], Deepak Nanjappa[21], Isabel C. Nimmo[2], Luke Noble[39,**], Anna M.G. Novák Vanclová[30], Mariusz Nowacki[17], Isaac Nuñez[23], Arnab Pain[40,41], Angela Piersanti[36], Sandra Pucciarelli[36], Jan Pyrih[1,24,30], Joshua S. Rest[42], Mariana Rius[19], Deborah Robertson[43], Aldane Ruaud[23], Iñaki Ruiz-Trillo[4,44,45], Monika A. Sigg[12], Pamela A. Silver[46,47], Claudio H. Slamovits[15], Estienne Swart[17,&], G. Jason Smith[48], Brittany Sprecher[35], Rowena Stern[9], Tobias von der Haar[24], Lev Tsypin[49,50], Aaron Turkewitz[49], Jernej Turnšek[6,7,46,45],

Matus Valach[16], Valérie Vergé[13], Peter von Dassow[23,51], Anastasios Tsaousis[24,25], Ross F. Waller[2], Lu Wang[52], Xiaoxue Wen[10], Glen Wheeler[9], April Woods[48], Huan Zhang[35], Thomas Mock[32,*], Alexandra Z. Worden[5,53,*] & Julius Lukeš[1,*]

[#]Equal contribution

[*]Corresponding authors: dranov@paru.cas.cz (DF); t.mock@uea.ac.uk (TM); azworden@geomar.de (AZW); jula@paru.cas.cz (JL)

[1]*Institute of Parasitology, Biology Centre, Czech Academy of Sciences and Faculty of Sciences, University of South Bohemia, České Budějovice, Czech Republic*

[2]*Department of Biochemistry, University of Cambridge, Cambridge, UK*

[3]*Bigelow Laboratory for Ocean Sciences, East Boothbay, USA*

[4]*Institut de Biologia Evolutiva, CSIC-Universitat Pompeu Fabra, Barcelona, Spain*

[5]*Monterey Bay Aquarium Research Institute, Moss Landing, USA*

[6]*Integrative Oceanography Division, Scripps Institution of Oceanography, University of California, San Diego, USA*

[7]*Microbial and Environmental Genomics, J. Craig Venter Institute, La Jolla, USA*

[8]*Molecular, Cell and Developmental Biology, University of California, Santa Cruz, USA*

[9]*The Marine Biological Association, Plymouth, UK*

[10]*School of Biological Sciences, University of Nebraska, Lincoln, USA*

[11]*Gordon and Betty Moore Foundation, Palo Alto, USA*

[12]*Department of Molecular and Cell Biology, University of California, Berkeley, USA*

[13]*Sorbonne Université, CNRS UMR7621, Observatoire Océanologique, Banyul sur Mer, France*

[14]*Institute de Biologie de l'ENS, Département de biologie, École Normale Supérieure, CNRS, INSERM, Paris, France*

[15]*Centre for Comparative Genomics and Evolutionary Bioinformatics, Dalhousie University, Halifax, Canada*

[16]*Department of Biochemistry and Robert-Cedergren Centre for Bioinformatics and Genomics, Université de Montréal, Montreal, Canada*

[17]*Institute of Cell Biology, University of Bern, Bern, Switzerland*

[18]*Center for Tropical and Emerging Global Diseases, University of Georgia, Athens, USA*

[19]*School of Marine and Atmospheric Sciences, Stony Brook University, Stony Brook, USA*

[20]*Department of Botany, University of British Columbia, Vancouver, Canada*

[21]*University of Delaware College of Earth, Ocean and Environment, Lewes, USA*

[22]*Woods Hole Oceanographic Institution, Woods Hole, MA, USA*

[23]*Facultad Ciencias Biológicas, Pontificia Universidad Católica de Chile, Fondo de Desarrollo de Areas Prioritarias, Center for Genome Regulation and Millennium Institute for Integrative Biology, Santiago de Chile, Chile*

[24]*School of Biosciences, University of Kent, Canterbury, Kent, UK*

[25]*Laboratory of Molecular and Evolutionary Parasitology, University of Kent, UK*

[26]*Graduate School of Life and Environmental Sciences, University of Tsukuba, Ibaraki, Japan*

[27]*Department of Mechanical Engineering, Massachusetts Institute of Technology, Boston, USA*

[28]*Department of Organismic and Evolutionary Biology, Harvard University, Cambridge, USA*

[29]*Centre for Organismal Studies, University of Heidelberg, Heidelberg, Germany*

[30]*Department of Parasitology, Faculty of Science, Charles University, BIOCEV, Vestec, Czech Republic*

[31]*Faculty of Life and Environmental Sciences, University of Tsukuba, Ibaraki, Japan*

[32]*School of Environmental Sciences, University of East Anglia, Norwich, UK*

[33]*Graduate School of Life Sciences, Tohoku University, Sendai, Miyagi, Japan*

[34]*Division of Environmental Photobiology, National Institute for Basic Biology, Okazaki, Aichi, Japan*

[35]*Department of Marine Sciences, University of Connecticut, Groton, USA*

[36]*School of Biosciences and Veterinary Medicine, University of Camerino, Camerino, Italy*

[37]*Department of Basic Biology, School of Life Science, Graduate University for Advanced Studies, Okazaki, Aichi, Japan*

[38]*Instituto de Biología Molecular y Celular, Universidad Nacional de Rosario, Rosario, Argentina*

[39]*Center for Genomics and Systems Biology, New York University, New York, USA*

[40]*Biological and Environmental Science and Engineering Division, King Abdullah University of Science and Technology, Thuwal, Jeddah, Saudi Arabia*

[41]*Center for Zoonosis Control, Global Institution for Collaborative Research and Education, Hokkaido University, Sapporo, Japan*

[42]*Department of Ecology and Evolution, Stony Brook University, Stony Brook, USA*

[43]*Lasry Center for Biosciences, Clark University, Worcester, USA*

[44]*Departament de Genètica Microbiologia i Estadıśtica, Universitat de Barcelona, Barcelona, Catalonia, Spain.*

[45]*Catalan Institution for Research and Advanced Studies, Barcelona, Catalonia, Spain.*

[46]*Department of Systems Biology, Harvard Medical School, Boston, USA*

[47]*Wyss Institute for Biologically Inspired Engineering, Harvard University, Boston, USA*

[48]*Department of Environmental Biotechnology, Moss Landing Marine Laboratoriess, Moss Landing, USA*

[49]*Department of Molecular Genetics and Cell Biology, University of Chicago, Chicago, USA*

[50]*Department of Biology, California Institute of Technology, Pasadena, USA*

[51]*Instituto Milenio de Oceanografia de Chile, Santiago de Chile, Chile*

[52]*Institute of Oceanography, Minjiang University, Fuzou, China*

[53]*Ocean EcoSystems Biology Unit, Marine Ecology Division, Helmholtz Centre for Ocean Research, Kiel, Germany*

[$]Present address: *AGADA Biosciences Inc., Halifax, Canada*

[**]Present address: *Institute de Biologie de l'ENS, Département de biologie, École Normale Supérieure, CNRS, INSERM, Paris, France*

[&]Present address: *Max Planck Institute of Developmental Biology, Tubingen, Germany*

ABSTRACT

Marine microbial eukaryotes underpin the largest food web on the planet and influence global biogeochemical cycles that maintain habitability. They are also remarkably diverse and provide insights into evolution, including the origins of complex life forms, as revealed through genome analyses. However, their genetic tractability has been limited to a few species that do not represent the broader diversity of eukaryotic life or some of the most environmentally relevant taxa. Here, we report on genetic systems developed as a community resource for experimental cell biology of marine protists from across the eukaryotic tree of life. We outline DNA delivery methods, expression constructs, and genome editing approaches that proved successful, as well as results from taxa where a working system was not achieved. The reported breakthroughs on genetic manipulation position the community to dissect cellular mechanisms from a breadth of

protists, which will collectively provide insights into ancestral eukaryotic lifeforms, protein diversification and evolution of cellular pathways.

INTRODUCTION

The ocean represents the largest continuous planetary ecosystem, hosting an enormous variety of organisms. These range from some of the largest creatures on Earth to a vast microscopic biota including unicellular eukaryotes (protists). Despite their small size, protists play key roles in marine biogeochemical cycles and harbor tremendous evolutionary diversity[1-3]. Notwithstanding their significance for understanding the evolution of life on Earth and their role in marine food webs, as well as driving biogeochemical cycles to maintain habitability, little is known about their cell biology including reproduction, metabolism, and signalling[4]. Most of the biological information available is based on comparison of proteins from cultured genome-sequenced species to homologs in genetically tractable model taxa, such as yeast[5-9]. A major impediment to understanding the cell biology of these diverse eukaryotes is that protocols for genetic modification are only available for a small number of species that represent neither the most ecologically relevant marine protistan species nor the breadth of eukaryotic diversity.

The development of genetic tools requires reliable information about gene organization and regulation of the emergent model species. Over the last decade, some of this information has become available through genome[5,6,8,10] and transcriptome sequencing initiatives[7,9,11,12] resulting in nearly 120 million unigenes from protists[13]. Insights from these projects have enabled the phylogenetically-informed approach[7] used herein for selecting and developing key marine protists into model systems. Forty-one scientific groups took part in a community-based effort resulting in the development of genetic tools that significantly expand the number of

eukaryotic lineages, which can be manipulated, and which encompass multiple ecologically important marine protists. These genetic tools transform our ability to address questions about the evolution and cell biology of these microorganisms and, by extension, other eukaryotes.

Here, we summarize detailed methodological achievements by this collaborative effort and analyse results to provide a synthetic 'Transformation Roadmap' for creating new microeukaryotic model systems. Although the organisms reported here are diverse, the paths to overcome difficulties share similarities, highlighting the importance of building a well-connected community to overcome technical challenges and accelerate the development of genetic tools. The new model species presented herein will not only extend our knowledge of cell biology and functional biodiversity, but also serve as platforms to advance microbial biotechnology.

RESULTS

Overview of studied organisms

Taxa were selected from multiple eukaryotic supergroups[1,7] to maximize the potential to compare fundamental aspects of cellular biology and to evaluate the numerous "hypothetical" unigenes found in marine protists **(Fig. 1)**. Previously, reproducible transformation of marine protists was limited to only a few species such as *Thalassiosira pseudonana*, *Phaeodactylum tricornutum*, and *Ostreococcus tauri* (**Supplementary Table 1**). Our initiative included 40 species, specifically, 6 Archaeplastida, 2 Haptophyta, 2 Rhizaria, 10 Stramenopila, 12 Alveolata, 4 Discoba, and 4 Opisthokonta (**Fig. 1**). Most of them were isolated from coastal habitats, the focus area of several major culture collections[7]. More than 50% of the selected species are considered photoautotrophs, with another 35% divided between heterotrophic osmotrophs and phagotrophs, the remainder being predatory mixotrophs. Almost 20% of the

chosen species are symbionts and/or parasites of marine plants or animals, 5% are associated with detritus, and several are responsible for harmful algal blooms (**Supplementary Table 2**). The main challenge of this initiative was to develop reverse genetics tools applicable to transforming all of these species, which not only require different cultivation conditions but are also phenotypically extremely diverse.

Roadmap for establishing new model organisms

The research teams met and conversed over a three-year period to identify and optimize the steps required to create new model systems (**Fig. 2**). Selectable markers, transformation conditions, and reporters were compared across species (**Supplementary Tables 3, 4 and 5**), and efforts were detailed using consistent terminology (**Table 1; Fig. 3; Fig. 4**). Information on partially successful or failed approaches was also summarized (see **Supplementary Results**) to facilitate future research efforts.

For some of the selected species, the first step was to identify cultivation conditions for robust growth in the laboratory and compatibility with transformation protocols. The aim was to generate axenic cultures and establish conditions supporting either high cell densities or large culture volumes to obtain sufficient amounts of biomass for use with a variety of molecular biology methods. Unlike established microbial model species, cultivation of marine protists can be challenging, especially for predatory taxa that require co-cultivation with their prey. Subsequent steps included the identification of suitable antibiotics and their corresponding selectable markers (**Supplementary Table 3**), conditions for introducing exogenous DNA (**Supplementary Table 4**), and selection of promoter and terminator sequences for designing transformation vectors (**Fig. 2; Supplementary Table 5**).

A variety of methods were used to test whether exogenous DNA was integrated into the genome or maintained as a plasmid and whether the introduced genes were expressed. Approaches to show the former included inverse PCR, Southern blots and whole genome sequencing, whereas approaches to demonstrate the latter included RT-PCR, epifluorescence microscopy, fluorescence-activated cell sorting (FACS), antibody-based methods, and growth assays in the presence of antibiotics to confirm transcription and translation of introduced selection and reporter genes (e.g., eGFP, YFP, mCherry). Transformation outcomes for each species were parsed into three groups according to the level of success or lack thereof and are discussed below according to their phylogenetic position (**Fig. 1**).

Archaeplastids

Prasinophytes are important marine green algae distributed from polar to tropical regions. They form a sister group to chlorophyte algae, and together, these two groups branch adjacent to land plants, collectively comprising the Viridiplantae, which are part of the Archaeplastida[1,8] (**Fig. 1**). Genome sequences are available for the picoprasinophytes (<3 µm cell diameter) tested herein, specifically, *Micromonas commoda*, *Micromonas pusilla*, *Ostreococcus lucimarinus* and *Bathycoccus prasinos*. A homologous recombination system exists for *Ostreococcus tauri*[14], which we extend here to *O. lucimarinus*. Additionally, we introduced the first genetic system(s) for *Bathycoccus*, a scaled, non-motile genus, and *Micromonas*, a motile, naked genus with larger genomes than *Bathycoccus* and *Ostreococcus*[8].

O. lucimarinus (RCC802) and *B. prasinos* (RCC4222) were transformed using protocols adapted from *O. tauri*[15]. Briefly, using electroporation (**Supplementary Table 4**) for transfer of exogenous genes, *O. lucimarinus* was transformed using a DNA fragment encoding the *O. tauri* high-affinity phosphate transporter (HAPT) gene fused to a luciferase gene and a KanMX

selection marker, which resulted in transient luciferase expression 24 h after electroporation (**Table 1; Supplementary Fig. 1**). After 2 weeks of growth in low melting agarose plates containing neomycin (1 mg/ml), 480 colonies were obtained, picked, and grown in artificial seawater with neomycin. Of these, 76 displayed luminescence ≥ 2.5 fold above background (80 Relative Luminescence Units, RLU), with widely variable levels (200 to 29100 RLU), likely reflecting either the site of integration and/or the number of integrated genes (**Supplementary Fig. 1**). The *O. tauri* construct did not work in *B. prasinos*, while the use of the *B. prasinos* histone H4 and high affinity phosphate transporter sequences in an otherwise identical construct and conditions was successful. Although luciferase expression was not detected 24 h after electroporation, 48 neomycin-resistant colonies were obtained 2 weeks later, 20 being luminescent when grown in liquid medium. Analysis of 14 resistant transformants revealed that the luciferase sequence was integrated into the genome of 5 clones that were luminescent, and one non-luminescent clone, suggesting that the chromatin context at integration sites in the latter was not favourable to luciferase expression (**Fig. 4A**).

The above methods for *Bathycoccus* and *Ostreococcus* failed in *Micromonas*. However, Lonza nucleofection was successful with *M. commoda* (CCMP2709) (**Table 1; Fig. 4B**) using 2 codon-optimized plasmids, one encoding the luciferase gene (NanoLuc, Promega) flanked by an exogenous promoter and terminator sequence from the 5′- and 3′- untranslated regions (UTRs) of histone H3 in *M. polaris*[8], and the other encoding an eGFP gene flanked by endogenous promoter and terminator sequences from the ribosomal protein S9. Acclimated mid-exponential *M. commoda* cells grown in L1 medium at 21 ºC were spun at 5000 x *g* for 10 min, the pellet was resuspended in Buffer SF (Lonza) premixed with carrier DNA (pUC19) and the plasmid, and 3 x 10^7 cells were used per reaction. After applying the EW-113 pulse, 100 µl of ice-cold recovery buffer (10 mM HEPES-KOH, pH 7.5; 530 mM sorbitol; 4.7% [w/v]

PEG 8000) was added to each well and incubated for 5 min at room temperature. Each reaction was then transferred into 2 ml L1, placed at 21 °C and light was increased stepwise over 72 h. Sensitivities to antibiotics were established (**Supplementary Table 3**). Constructs did not include a selectable marker, as we aimed to introduce and express foreign DNA while developing conditions suitable for transfection that supported robust growth in this cell wall-lacking protist. Transformants revealed a significantly higher level of eGFP fluorescence than wild type cells, with 1.3% of the population showing fluorescence per cell 45-fold higher than both the non-transformed portion of the culture and the wild type cells (**Fig. 4B**). Additionally, the RLU was 1500-times higher than controls when using the luciferase-bearing construct, such that multiple experiments with both plasmids confirmed expression of exogenous genes in *M. commoda*.

***Haptophytes* (incertae sedis)**

Haptophytes are a group of photosynthetic protists that are abundant in marine environments and include the major calcifying lineage, the coccolithophores. Genome sequences are available for *Emiliania huxleyi*[6] and *Chrysochromulina tobin*[16], and there are few reports of nuclear transformation of haptohytes[17]. Here, a stable nuclear transformation system was developed for *Isochrysis galbana*, a species that lacks coccoliths, but represents an important feedstock for shellfish aquaculture[18].

I. galbana (CCMP1323) was transformed by biolistic bombardment with the pIgNAT vector, which contains nourseothricin *N*-acetyltransferase (NAT, for nourseothricin resistance) driven by the promoter and terminator of Hsp70 from *E. huxleyi* (CCMP1516). Twenty four hours after bombardment, cells were transferred to liquid f/2 medium at 50% salinity containing 80 µg/ml nourseothricin (NTC) and left to grow for 2-3 weeks to select for transformants (**Table**

1). The presence of NAT in NTC-resistant cells was verified by PCR and RT-PCR (**Fig. 4C)** and the sequence verified. To confirm NTC resistance was a stable phenotype, cells were sub-cultured every 2-4 weeks at progressively higher NTC concentrations (up to 150 µg/ml NTC) in the above-mentioned media. Cells remained resistant to NTC for approximately 6 months, as confirmed by PCR screening to identify the presence of the NAT gene.

Rhizarians

Rhizarians include diverse non-photosynthetic protists, as well as the photosynthetic chlorarachniophytes that acquired a plastid *via* secondary endosymbiosis of a green alga. Uniquely, they represent an intermediate stage of the endosymbiotic process, since their plastids still harbor a relict nucleus (nucleomorph)[5]. Here, we have advanced a transformation protocol for the chlorarachniophyte *Amorphochlora (Lotharella) amoebiformis* for which low-efficiency transient transformation has previously been achieved using particle bombardment[19].

A. amoebiformis (CCMP2058) cells (1 x 10^7) were resuspended in 100 µl of Gene Pulse Electroporation Buffer (BioRad) with 20 to 50 µg of the reporter plasmid encoding GFP-RubisCO fusion protein under the control of the native rbcS1 promoter and subjected to electroporation (**Supplementary Table 4**). Cells were immediately transferred to fresh ESM medium and incubated for 24 h. Transformation efficiency was estimated by the fraction of cells expressing eGFP, resulting in 0.03-0.1% efficiency, as enumerated by microscopy, showing an efficiency up to 1,000-fold higher than the previous study[19] (**Table 1**). Stable transformants were generated by manual isolation using a micropipette, and a transformed line has maintained eGFP fluorescence for at least 10 months without antibiotic selection (**Fig. 3**).

Stramenopiles

Stramenopiles are a diverse lineage with many important photoautotrophic, mixotrophic and heterotrophic taxa. As the most studied class in this lineage, diatoms (Bacillariophyceae) were early targets[20,21] for the development of reverse genetics tools. Diatoms alone are estimated to contribute approximately 20% of annual carbon fixation[22] and, like several other algal lineages, are used in bioengineering applications, such as the production of high-value end products and biofuels[23]. The work presented here builds on established reverse genetics tool for diatoms[21] and recently developed for conjugation-based DNA delivery[24] and genome editing[25,26]. An improved method for episome-based and CRISPR/Cas-driven gene knockout is presented for *P. tricornutum* (see **Supplementary Results**) More efficient *T. pseudonana* conjugation-based DNA delivery is also described. New transformation protocols are presented for *Fragilariopsis cylindrus*, the first cold-adapted alga to have such a system, as well as the coastal species *Pseudo-nitzschia multiseries* (producer of the neurotoxin domoic acid) and *Pseudo-nitzschia australis.* We also present the first successful transformations for other marine stramenopile groups. Specifically, for *Nannochloropsis oceanica*, a photosynthetic eustigmatophyte and for the non-photosynthetic labyrinthulomycete *Aurantiochytrium limacinum*. All of these stramenopiles except *P. australis* have a sequenced genome[27].

Microparticle bombardment was used on *F. cylindrus* (CCMP1102), grown and maintained at 4 °C during the protocol. Exponential phase cells (5 x 10^7) were harvested onto a 1.2 µm membrane filter (Millipore) which was then placed on an 1.5% agar Aquil plate for bombardment with beads coated with a plasmid containing zeocin resistance and eGFP, both controlled by an endogenous fucoxanthin chlorophyll *a/c* binding protein (FCP) promoter and terminator (**Table 1; Supplementary Tables 3 and 4**)[28]. Transformation was performed using 0.7 µm tungsten particles and the biolistic particle delivery system PDS1000/He (BioRad).

Rupture discs for 1,350 and 1,550 pounds per square inch (psi) gave the highest colony numbers (efficiencies of 20.7 colony forming units (cfu)/10^8 cells and 30 cfu/10^8 cells, respectively. Following bombardment, the filter was turned upside down and left to recover (24 h) on the plate, then cells were rinsed from the plate/filter and spread across five 0.8% agar Aquil plates with 100 µg/ml zeocin. Colonies appeared 3 to 5 weeks later. PCR on genomic DNA showed that 100% and 60% of colonies screened positive for the zeocin resistance and eGFP genes, respectively. Confirmed by FACS and microscopy, eGFP was localized to the cytosol and was distinguishable from plastid autofluorescence (**Fig. 3**). Both genes were present in transformants after multiple transfers (> 10) 2 years later, indicating long-term stability.

We selected the silaffin precursor TpSil3p (**Table 1**) as the target gene for improving bacterial conjugation in *T. pseudonana* (CCMP1335). TpSil3p was fused to eGFP flanked by an FCP promoter and terminator, cloned into pTpPuc3 episomal backbone, and transformed into mobilization plasmid-containing EPI300 *E. coli* cells (Lucigen). The donor cells were grown in SOC medium at 37 °C until OD_{600} of 0.3–0.4, centrifuged and resuspended in 267 µl SOC medium. Next, 200 µl donor cells were mixed with 4 x 10^7 *T. pseudonana* cells, co-cultured on pre-dried 1% agar plates, dark incubated at 30 °C for 90 min, then at 18 °C in constant light for 4 h, followed by selection in 0.25% agar pour plates containing 100 µg/ml nourseothricin. Colonies were observed after 2 weeks, inoculated into 300 µl L1 medium and supplemented with 200 µg/ml nourseothricin to reduce the number of false positives. Positive transformants were identified by colony PCR screening (**Supplementary Fig. 2**) and epifluorescence microscopy (**Fig. 3**).

The diatoms *Pseudo-nitzschia multiseries* (15093C) and *P. australis* and other members of this genus form buoyant linear chains with overlapping cell tips during active growth, and were

unconducive to punctate colony formation on agar, where their growth is generally poor. A low-gelation-temperature agarose seawater medium (LGTA) was developed to facilitate growth, antibiotic selection, and cell recovery. Both diatoms exhibited growth inhibition at relatively low concentrations under nourseothricin, formaldehyde, and zeocin (**Supplementary Table 3**). Biolistic transformation of two other *Pseudo-nitzschia* species had been demonstrated at low efficiency[29]. To complement this approach and explore potentially higher efficiency methods for transformation with diatom episomal plasmids, we modified the existing conjugation-based method[24]. The published conjugation protocol was modified to enhance *P. multiseries* post-conjugation viability by reducing SOC content. An episomal version of the Pm_actP_egfp_actT expression cassette was transfected into *E. coli* EPI300+pTAMOB and used for conjugation. After 48 h in L1 medium, cells were plated in LGTA and eGFP-positive cells were observed 7 days later (**Fig. 3**). PCR revealed the presence of plasmids in all eGFP positive colonies. Similarly, conjugation with the episome pPtPUC3 (bleomycin selection marker)-containing bacterial donors was followed under zeocin selection (200 μg/ml). After 7 days, only viable cells (based on bright chlorophyll fluorescence) contained the episome, as confirmation by PCR. Propagation of transformants after the first medium transfer (under selection) has so far been unsuccessful.

The electroporation of *N. oceanica* (CCMP1779) was optimized based on the ability to treat cells with fluorescein-conjugated 2000 kDa dextran and their subsequent survival (**Supplementary Table 4**). Increasing the sorbitol concentration to 800 mM and electroporating at between 5 and 9 kV/cm resulted in highest cell recovery. This protocol was used to introduce plasmids containing the gene for the blue fluorescent reporter mTagBFP2 under control of the cytomegalovirus (CMV), the cauliflower Mosaic Virus 35S, or the VCP1 promoter previously described from *Nannochloropsis* sp.[30]. Transient expression of blue

fluorescence (compared to cells electroporated simultaneously with the same protocol without plasmid) appeared within 2 h, lasted for at least 24 h, and disappeared by 48 h in subsets of cells electroporated with mTagBFP2 under the control of CMV (**Fig. 4D).** The effectivness of transient transformation was much higher when a linearized plasmid was used compared to a cirular plasmid (**Table 1**). VCP1 did not induce blue fluorescence with a circular plasmid, while 35S gave inconsistent results when both circularized and linearized plasmids were used.

Stable transformation of *A. limacinum* (ATCC MYA-1381 or NIBH SR21) was achieved by knock-in of a resistance cassette composed of the bleomycin-resistance gene (shble) driven by 1.3 kb promoter and 1.0 kb terminator regions of the endogenous glyceraldehyde-3-phosphate dehydrogenase gene carried in a pUC19-based plasmid (18GZG) along with the native 18S rRNA gene, and by knock-in of a similar construct containing a yeGFP:shble fusion (18GeZG) (**Supplementary Fig. 3**). Approximately 1 x 10^8 cells were electroporated (**Supplementary Table 4**), adapting the electroporation protocol used for *Schizochytrium*[31]. The highest transformation efficiency was achieved using 1 µg of linearized 18GZG plasmid with 2 pulses, resulting in a time constant of ~5 ms (**Supplementary Table 4**). Expression of the fusion protein was confirmed by both the zeocin-resistance phenotype and the detection of eGFP (**Fig. 3**). Six 18GZG transformants derived from uncut and linearized plasmids were examined in detail. All maintained antibiotic resistance throughout 13 serial transfers, first in selective, and subsequently in non-selective media, and then again in selective medium. Integration of the plasmid into the genome was confirmed by PCR as well as by Southern blots using a digoxigenin-labeled shble gene probe, showing that 4 transformants had integrations by single homologous recombination, while in 2 transformants, additional copies of the antibiotic resistance cassette were integrated by non-homologous recombination elsewhere in the genome (**Supplementary Fig. 3**).

Alveolates

This species-rich and diverse group is subdivided into ciliates, apicomplexans, and dinoflagellates (**Fig. 1**). As a link between apicomplexan parasites and dinoflagellate algae, perkinsids are key for understanding the evolution of parasitism, and also have potential biomedical applications. Techniques currently exist for transformation of only a small number of ciliates, perkinsids and apicomplexans[32,33]. Here, we present results for the perkinsid *Perkinsus marinus*, a major pathogen of marine mollusks, fish, and amphibians[34]. Additionally, advances in transformation methods were made for 4 dinoflagellate species: *Oxyrrhis marina,* a basal-branching phagotroph that lacks photosynthetic plastids, *Crypthecodinium cohnii,* a heterotroph used in food supplements, *Amphidinium carterae* with a highly reduced plastid genome containing only a small number of genes encoding proteins for photosynthetic electron transport, rRNAs and one tRNA, and *Karlodinium veneficum,* a mixotroph (combining photosynthetic and phagotrophic nutrition) that produces fish-killing karlotoxins[35].

We advanced the *P. marinus* (PRA240) transformation system[36,37] using a newly formulated transformation 3R buffer (200 mM Na_2HPO_4; 70 mM NaH_2PO_4; 15 mM KCl; 1.5 mM $CaCl_2$; 150 mM HEPES-KOH, pH 7.3) that makes the electroporation reactions cheaper and therefore more accessible. We were able to co-express 2 genes and efficiently select transient and stable transformants using FACS (**Fig. 3; Table 1**). In addition, we established the integration profile of ectopic DNA once introduced into the *P. marinus* genome. We saw no evidence of integration through homologous recombination, and a propensity for plasmid fragmentation and integration within transposable elements sites. Furthermore, an optimized alternative protocol for transformation using glass bead abrasion was developed. In brief, 5 x 10^7 cells were resuspended in 330 µl of fresh ATCC Medium 1886 and were mixed with 5.0 µg of

linearized and circular [1:1] plasmid and 300 µl of glass beads (Sigma) in a 1.5 ml tube, vortexed for 30 s at maximum speed, and the cells in 500 µl of culture medium were transferred to 6-well plates in a final volume of 3 ml. Two versions of the previously published Moe gene promoter were tested[36]. Whereas the 1.0 kb promoter version induced expression after 2 or 3 days, the truncated version (0.5 kb) took 7 days for expression to be detected. Resistance genes to bleomycin, blasticidin and puromycin have all been shown to confer resistence to transformed *P. marinus*; however, selection regimes are still relatively slow and inefficient, indicating further room for improvement[37].

O. marina (CCMP1788) was cultured in f/2 medium with a diverse bacterial community and fed weekly with heat-killed *E. coli*. Selection trials revealed that 5 different antibiotics led to 100% mortality of *O. marina* in 6 days (**Supplementary Table 3**). Fluorescently-labelled DNA or DNA analogs such as FITC dextran were used to test the efficiency of delivery using a variety of chemical or electrical methods. For instance, incubation with $CaCl_2$ allowed introduction of Alexa 488-labeled DNA (Molecular Probes) with 20% efficiency. Briefly, a mix of 1 to 8 µg of DNA and $CaCl_2$ (f.c. 0.25 M) was combined with an equal volume of HeBS (274 mM NaCl; 10 mM KCl; 1.4 mM Na_2HPO_4; 15 mM D-glucose; 42 mM HEPES, pH 7.1) and incubated with 1 ml of *O. marina* culture. FITC-dextran incorporation was achieved when using Gene Pulser Electroporation Buffer in combination with three 5 ms square-wave pulses (0.1 ms pause between pulses) using a field strength of 0.5 kV/cm (**Supplementary Table 4**). Transient expression of mCherry was observed after introducing a plasmid encoding mCherry gene with a flanking sequence of the hsp90 gene from *O. marina* using the transformation protocol from above (**Fig. 3; Table 1**).

The cell cycle of *C. cohnii* consists of motile G1 cells, which encyst when they shed their

flagella completing the remaining cell-cycle phases[38]. After cytokinesis, the daughter cells remain inside the mother cell, and in this stage, treatment with PEG results in the release of the non-motile spheroplasts[39]. Transfection of *C. cohnii* (CCMP316) was attempted using physical (electroporation, microfluidics, particle bombardment) and chemical (lipofection) methods in motile daughter cells and spheroplasts with both electroporation and lipofection resulting in DNA delivery. *C. cohnii* spheroplasts were electroporated with 5 µg of plasmid using Amaxa Cell Line Optimization Solution V or 3R buffer and program D-023 in Nucleofector (Lonza). The swimming cells and spheroplasts were resuspended in 1 mg of FITC-Dextran and 300 µl of glass beads, vortexed at maximum speed for 15-30 s and subsequently recovered in fresh medium. Biolistics was also tried on 2.5 x 10^7 swimming cells and spheroplast using 7.5 µg of HEM plasmid, FITC-dextran, 3 µg of Cas9/sgRNA and 7.5 µg of GFP-carrying plasmid. Cells were precipitated in the presence of gold beads and shooting was carried out in a vacuum at >25 Hg using a 1550 psi rupture disk. Plasmids from *P. marinus* (PmMOE:GFP-11)[36], *Hematodinium* sp. (UB-GFP and EF-GFP) under human ubiquitin promoters, PAY and PAYCO using *E. huxleyi* ubiquitin promotors, purified Cas9 protein with synthetic sgRNA and donor DNA template with the GFP gene and site-directing homology flanking sequences resulted in no fluorescent cells independently of the delivery method attempted. We also tested transformation using chemically labeled DNA (Alexa Fluor 488) and FITC-labeled 150 kDa dextran. *C. cohnii* withstands electroporation with low or no damage, and its swimming cells were difficult to disrupt with glass-bead abrasion and particle bombardment, whereas spheroplasts were much more sensitive. Electroporation of spheroplasts was successful using the Lonza program X-001 or lipofection, both with labeled DNA (**Fig. 3**), but expression of encoded genes was not confirmed and the number of transfected cells was very low. We also attempted electroporation and microfluidics (5 square waves and 6 exponential decays)[40] with plasmids PmMOE:GFP-11, UB-GFP, EF-GFP, PAY and PAYCO but with no positive

outcome.

For *A. carterae* (CCMP1314), we successfully conducted transformation of plastid DNA. In brief, we selected psbA (encodes D1 of photosystem II), which is a target of the herbicide atrazine (**Supplementary Table 3**). Two shuttle vectors using an *E. coli* plasmid backbone, both based on the psbA minicircle, were constructed. One introduced a mutation in the psbA gene to confer atrazine resistance (pAmpPSBA) and in the other vector psbA was replaced by chloramphenicol acetyl transferase (CAT; pAmpChl). While no transformants were seen for glass-bead agitation, NEPA electroporation or Lonza nucleofection, biolistic transformation with DNA-coated gold microparticles rendered transformed cells. Those with pAmpPSBA were not stable long-term; however, the pAmpChl transformants were stable for at least 12 months, and RT-PCR (**Fig. 4E**) showed that the CAT gene was transcribed[41], albeit missing the polyU tail which is normally added post-transcriptionally to all *A. carterae* plastid transcripts. Attempts to transform *Symbiodinium microadriaticum* using the same approach were unsuccessful[42].

Since *K. veneficum* (CCMP1975) is sensitive to kanamycin (**Supplementary Table 3**), a neomycin resistance gene (Neo) was added to the backbone of a dinoflagellate-specific expression vector[43], named DinoIII-Neo. After linearization, the vector was successfully electroporated by Nucleofector (Lonza). The preprogrammed Nucleofector optimization pulse codes, buffer SF/Solution I (Lonza), and 2 μg/μl of linearized DinoIII-Neo were used. Electroporated cells were selected under 150 μg/ml kanamycin 3 days post-electroporation. New seawater with kanamycin was added every 2 weeks to the cultures and new subcultures were inoculated monthly. Total RNA was isolated and cDNA synthesized as previously reported[44] using random hexamer as the primer. Out of 16 pulse codes tested, CA-137 and DS-

138 resulted in long-term survival of *K. veneficum* under kanamycin selection. CA-137 resulted in high cell densities for several months, with the resistance gene successfully detected by PCR (**Fig. 4F**).

Discobans

This diverse group, recently split into Discoba and Metamonada[45], includes heterotrophs, photoautotrophs, predatory mixotrophs, as well parasites. The Discoba include parasitic kinetoplastids with clinical significance, such as *Trypanosoma brucei*, *T. cruzi* and *Leishmania* spp., for which efficient transformation protocols are available[46]. However, such protocols are missing for marine species. Here, we describe transformation protocols for the kinetoplastid *Bodo saltans,* the diplonemid *Diplonema papillatum*, and the heterolobosean *Naegleria gruberi*.

B. saltans ('Lake Konstanz' strain) was transformed with a plasmid containing a cassette designed to fuse an endogenous EF-1α gene with GFP for C-terminal tagging. This cassette includes downstream GFP, a *B. saltans* tubulin intergenic region followed by the aminoglycoside 3'-phosphotransferase gene (Neo), conferring resistance to neomycin. EF-1α genes exist in tandem repeats; however, the homologous regions that flank the cassette to induce homology-directed repair were chosen to target only one copy of the gene. As transcription in *B. saltans* is polycistronic[47], insertion of the tubulin intergenic region into the plasmid is essential for polyadenylation of the EF1-α/GFP fusion and *trans*-splicing of the Neo gene. Square-wave electroporation (Nepa21) was used with a poring pulse of 250V (25 ms) and 5 transfer pulses of 60V (99 ms) in the presence of Cytomix buffer (120 mM KCl; 0.15 mM $CaCl_2$; 10 mM KH_2PO_4; 2 mM EGTA; 5 mM $MgCl_2$; 25 mM HEPES-KOH, pH 7.6). Selection of transfected cells began with 2 µg/ml of neomycin added 24 h after electroporation,

and gradually increased over 2 weeks to 5 μg/ml (**Table 1**). Cells were washed and subcultured into fresh selection medium every 4 days, and neomycin-resistant cells emerged 7 to 9 days post-electroporation. The GFP signal was detected 2 days post-electroporation, albeit with low intensity. This may be due to the inefficient translation of eGFP since it has not been codon-optimized for *B. saltans* (**Fig. 3**). Genotyping analysis 9 months post-transfection confirmed the presence of the Neo gene and at least partial plasmid sequence. However, plasmid integration into the *B. saltans* genome through homologous recombination is still unconfirmed. This suggests either off-target plasmid integration or that the plasmid is maintained episomally.

D. papillatum (ATCC 50162) was transformed by electroporation using 3 μg of *SwaI*-linearised fragment (cut from p57-V5+NeoR plasmid) containing V5-tagged Neo gene flanked by partial regulatory sequences derived from the hexokinase gene of the kinetoplastid *Blastocrithidia* (strain p57) (**Table 1**) using a published protocol[48]. About 18 h after electroporation, 75 μg/ml neomycin was added to the medium and after 2 weeks 7 neomycin-resistant clones were recovered. Transcription of Neo was verified in 2 clones by RT-PCR, and the expression of the tagged Neo protein was confirmed by Western blots using α-V5 antibody (**Fig. 4G**). As preliminary data indicate that the homologous recombination machinery is present and active in *D. papillatum,* extending the 5' and 3' homologous regions (> 1 kb) may increase integration efficiency.

For *N. gruberi* (ATCC 30224) two plasmids were designed. The first one carried the hygromycin-resistance gene with an actin promoter and terminator, along with an HA-tagged eGFP driven by the ubiquitin promoter and terminator. The second plasmid carried the Neo gene instead. For each individual circular plasmid, 4 μg was electroporated (**Supplementary Table 4**). About 48 h after electroporation, dead cells were removed from the suspension and

viable cells were washed with PBS. Afterwards, 300 μg/ml of hygromycin B or 700 μg/ml of neomycin was added to the fresh media (**Table 1**). One to 4 weeks later several resistant clones were recovered and expression of eGFP and/or hygromycin was confirmed by Western blots. Expression of eGFP was observed by epifluorescence microscopy (**Fig. 3**) with ~80% of transformants maintaining hygromycin or neomycin resistance in addition to expressing eGFP.

Opisthokonts

The opisthokont clade Holozoa includes animals and their closest unicellular relatives Choanoflagellata, Filasterea, Ichthyosporea, and Corallochytrea. The establishment of molecular genetic tools in non-metazoan holozoans promises to help illuminate the cellular and genetic foundations of animal multicellularity[9]. Genomic and transcriptomic data are available for multiple representatives characterized by diverse cell morphologies, some of which can even form multicellular structures[9,12]. Here, we show that transient transformations have been achieved for the filasterean *Capsaspora owczarzaki*[49], the ichthyosporean *Creolimax fragrantissima*[50] and the choanoflagellate *Salpingoeca rosetta*[51]. A novel protocol is presented for transforming the ichthyosporean *Abeoforma whisleri*, isolated from the digestive tract of mussels, and we have improved a transformation protocol for *S. rosetta*[51].

All *A. whisleri* life stages are highly sensitive to a variety of methods for transformation. We developed a Lonza 4D-nucleofection-based protocol using 16-well strips, wherein PBS-washed cells were resuspended in 20 μl of buffer P3 (Lonza) containing 40 μg of carrier plasmid (empty pUC19) and 1-5 μg of the reporter plasmid (*A. whisleri* H2B fused to mVenus fluorescent protein, mVFP) (**Table 1**), and subjected to code EN-138 (Lonza). Immediately after the pulse, cells were recovered by adding 80 μl of marine broth (Gibco) prior to plating

in 12-well culture plates previously filled with 1 ml marine broth. After 24 h, ~1% of the culture was transformed based on the fraction of cells expressing mVFP in the nucleus (**Fig. 3**).

As part of this initiative, we also developed a method for transiently transfecting the choanoflagellate *S. rosetta* using a modified protocol for Lonza nucleofection*51* (**Fig. 3**). Improvement to this protocol include the use of selection for expression of a puromycin resistance gene that enables stable transformation of *S. rosetta* and allows for genetic complementation (**Table 1**). Lessons from these efforts, including the use of the highly sensitive reporter nanoluc gene, a hypertonic recovery buffer and large amounts of carrier DNA helped with the establishment and improvement of transformation conditions for *Micromonas* sp. and *A. whisleri*, respectively.

DISCUSSION

Marine organisms play essential roles in global biogeochemical cycles and produce approximately half of the Earth's oxygen[1,22]. Decades of research by marine biologists, ecologists, protistologists, and oceanographers have contributed to an increasingly coherent picture of the oceanic ecosystem. These studies highlight the diversity of ocean life, including the protistan component[2,3]. Remarkable strides have also been made in developing an overview of the genomes and predicted proteomes of these protists[13]. However, without genetic manipulation systems, these taxa remain an untapped resource for providing deeper insights into their cell biology, with potentially valuable outcomes for evolutionary studies, nanotechnology, biotechnology, medicine, and pharmacology.

Global synthesis of the approaches developed herein provides a Transformation Roadmap that will guide future efforts to establish new and emergent model organisms (**Fig. 2**). Notably, our

studies did not result in a universally applicable protocol, likely because transformability and a range of other key conditions varied greatly across taxa and approaches. Factors influencing outcomes include intrinsic features of the genome (e.g., presence/absence of homologous recombination, extrachromosomal elements, genome size), as well as morphology and structural features of the cell. In general, electroporation proved the most common method for introducing exogenous DNA stably into the cell. This approach was utilized for naked cells and protoplasts, yet frequently also worked, albeit with lower efficiency, on cells protected by cell walls. Linearized plasmids were most effective for delivery, and 5' and 3' UTRs-containing promotors of highly expressed endogenous genes provided the strongest expression of selective reporters and markers.

Our results significantly expand the segment of extant eukaryotic diversity amenable to reverse genetics approaches. Out of the 40 microbial eukaryotes selected, we were able to deliver and express exogenous DNA in ca. 50% of them. This high rate of success testifies to the benefits of taking on high-risk research in a large, open, and collaborative context[52]. The new systems reported herein open a wealth of opportunities for exploring functional differences between members of relatively conserved protein families shared across eukaryotes, or even domains of life. These novel transformation systems also enable us for the first time to shed light on the function of species-specific genes which likely reflect key adaptations to specific niches in dynamic ocean habitats.

ACKNOWLEDGEMENTS

We thank M. Salisbury for assistance, C. Poirier and M. Hamilton (Monterey Bay Aquarium Research Institute) for FACS analysis; and Vinay K. Nagarajan, Monica Accerbi, and Pamela J. Green (University of Delaware) who carried out the *Agrobacterium* studies. We are grateful

to L. Teytelman from protocols.io. This collaborative effort was supported by the Gordon and Betty Moore Foundation EMS Program of the Marine Microbiology Initiative and other forms of grant support to the participating laboratories.

AUTHOR CONTRIBUTIONS

The project was conceived and designed by A.C.J., J.Z.K., S.B., D.F., J.L., R.E.R.N., J.A.F.R., E.C., L.S., A.Z.W., T.M., A.E.A., F.Y.B, C.B, Ch.B., H.C., T.C., J.L.C., K.C., C.L.D., V.E., V.H., Y.H., C.J.H., P.J.K., N.K., S.L., C.M., J.M., I.R.T., P.A.S., C.H.S., G.J.S., A.T., P.V.D., A.T. and R.F.W. Data analysis was carried out by M.A.J., C.A., C.B., A.C.B., P.B., D.S.B., S.A.B., A.B., G.B., R.C., M.A.C., D.B.C., L.C., R.D., E.E., P.A.E., F.F., V.F.B., N.J.F., K.F., P.A.G., P.R.G., F.G., S.G., J.G., Y.H., E.R.H.C., E.H., A.Hi., A.Ho., I.H., J.I., N.A.T.I., Y.I., N.E.J., A.K., K.F.K., B.K., E.K., L.A.K., N.L., I.L., Z.L., J.C.L., F.L., S.M., T.M., M.M., S.R.N., D.N., I.C.N., L.N., A.M.G.N.V., M.N., I.N., A.Pa., A.Pi., S.P., J.P., J.S.R., M.R., D.R., A.R., M.A.S., E.S., B.S., R.S.,T.V.H., L.T., J.T., M.V., V.V., L.W., X.W., G.W., A.W. and H.Z. The manuscript was written by D.F., R.E.R.N., J.A.F.R., E.C., L.S., T.M., A.Z.W. and J.L. with input from all authors.

COMPETING INTERESTS

The authors declare no competing interests.

REFERENCES

1. Worden, A.Z. et al. Rethinking the marine carbon cycle: Factoring in the multifarious lifestyles of microbes. *Science* **347**, 1257594 (2015).

2. de Vargas, C. et al. Eukaryotic plankton diversity in the sunlit global ocean. *Science* **348**, 1261605 (2015).
3. Duarte, C. M., Regaudie-de-Gioux, A., Arrieta, J. M., Delgado-Huertas, A. & Agustí, S. The oligotrophic ocean is heterotrophic. *Annu. Rev. Mar. Sci.* **5**, 551-569 (2013).
4. Collier, J. L. & Rest J. S. Swimming, gliding, and rolling toward the mainstream: cell biology of marine protists. *Mol. Biol. Cell.* **30**, 1245-1248 (2019).
5. Curtis, B. A., Tanifuji, G. & Burki, F. Algal genomes reveal evolutionary mosaicism and the fate of nucleomorphs. *Nature* **492**, 59–65 (2012).
6. Read, B.A. et al. Pan genome of the phytoplankton *Emiliania* underpins its global distribution. *Nature* **499**, 209-213 (2013).
7. Keeling P. J., Burki, F., Wilcox, H. M., Allam, B. & Allen, E. E. The Marine Microbial Eukaryote Transcriptome Sequencing Project (MMETSP): illuminating the functional diversity of eukaryotic life in the oceans through transcriptome sequencing. *PLoS Biol*. **12**, e1001889 (2014).
8. van Baren, M. J. et al. Evidence-based green algal genomics reveals marine diversity and ancestral characteristics of land plants. *BMC Genomics* **17**, 1–22 (2016).
9. Richter, D. J., Fozouni, P., Eisen, M. & King, N. Gene family innovation, conservation and loss on the animal stem lineage. *eLife* **7**, 1–43 (2018).
10. Strassert, J. F. H. et al. Single cell genomics of uncultured marine alveolates shows paraphyly of basal dinoflagellates. *ISME J.* **12**, 304-308 (2018).
11. Joseph, S. J. et al. The Alveolate *Perkinsus marinus*: Biological insights from EST gene discovery. *BMC Genomics* 11, 228 (2010).
12. Grau-Bové, X. et al. Dynamics of genomic innovation in the unicellular ancestry of animals. *eLife* **6**, e26036 (2017).

13. Carradec, Q., Pelletier, E., Da Silva, C., Alberti, A. & Seeleuthner, Y. A global atlas of eukaryotic genes. *Nat. Commun.* **9**, 373 (2018).

14. Lozano, J.-C. et al. Efficient gene targeting and removal of foreign DNA by homologous recombination in the picoeukaryote *Ostreococcus*. *Plant J.* **78**, 1073-1083 (2014).

15. Van Ooijen, G., Knox, K., Kis, K., Bouget, F-Y. & Millar, A. J. Genomic transformation of the picoeukaryote *Ostreococcus tauri*. *J. Vis. Exp.* **65**, e4074 (2012).

16. Hovde, B.T. et al. Genome sequence and transcriptome analyses of *Chrysochromulina tobin*: Metabolic tools for enhanced algal fitness in the prominent order Prymnesiales (Haptophyceae). *PLoS Genet.* **11**, e1005469 (2015).

17. Endo, H. et al. Stable nuclear transformation system for the coccolithophorid alga *Pleurochrysis carterae. Sci. Rep.* **6**, 22252 (2016).

18. Dörner, J., Carbonell, P., Pino, S. & Farias, A. Variation of fatty acids in *Isochrysis galbana* (T-Iso) and *Tetraselmis suecica*, cultured under different nitrate availabilities. *J. Fish. Aquacult.* **5**, 1-3 (2014).

19. Hirakawa, Y., Kofuji, R. & Ishida, K. Transient transformation of a chlorarachniophyte alga, *Lotharella amoebiformis* (chlorarachniophyceae), with uidA and egfp reporter genes. *J. Phycol*. **44**, 814–20 (2008).

20. Dunahay, T. G., Jarvis, E. E. & Roessler, P. G. Genetic transformation of the diatoms *Cyclotella cryptica* and *Navicula saprophila*. *J. Phycol.* **31**, 1004–1012 (1995).

21. Apt, K. E., Kroth-Pancic, P. G. & Grossman, A. R. Stable nuclear transformation of the diatom *Phaeodactylum tricornutum*. *Mol. Gen. Genet*. **252**, 572-579 (1996).

22. Field, C.B., Behrenfeld, M.J., Randerson, J.T. & Falkowski, P. Primary production of the biosphere: Integrating terrestrial and oceanic components. *Science* **281**, 237-240 (1998).

23. Mishra, M., Arukha, A. P., Bashir, T., Yadav, D. & Prasad, G.B.K.S. All new faces of diatoms: Potential source of nanomaterials and beyond. *Front. Microbiol.* **8**, 1239 (2017).

24. Karas, B. J. et al. Designer diatom episomes delivered by bacterial conjugation. *Nat. Commun.* **6**, 6925 (2015).

25. Nymark, M., Sharma, A. K., Sparstad, T., Bones, A. M. & Winge, P. A. CRISPR/Cas9 system adapted for gene editing in marine algae. *Sci. Rep.* **6**, 24951 (2016).

26. Hopes, A., Nekrasov, V., Kamoun, S. & Mock, T. Editing of the urease gene by CRISPR-Cas in the diatom Thalassiosira pseudonana. *Plant Methods* **12**, 49 (2016).

27. Mock, T. J. et al. Evolutionary genomics of the cold-adapted diatom *Fragilariopsis cylindrus*. *Nature* **541**, 536–540 (2017).

28. Kroth, P. G. Genetic Transformation; A tool to study protein targeting in diatoms. *Methods Mol. Biol.* **390**, 257–267 (2007).

29. Sabatino, V. et al. Establishment of genetic transformation in the sexually reproducing diatoms *Pseudo-nitzschia multistriata* and *Pseudo-nitzschia arenysensis* and inheritance of the transgene. *Marine Biotech.* **17**, 452-462 (2015).

30. Kilian, O., Benemann, C. S., Niyogi, K. K. & Vick, B. High-efficiency homologous recombination in the oil-producing alga *Nannochloropsis* sp. *Proc. Natl. Acad. Sci. USA* **108**, 21265-21269 (2011).

31. Ono, K., Aki, T. & Kawamoto, S. Method for introducing a gene into labyrinthulomycota. US Patent 7,888,123 (2011).

32. Donald, R. G. & Roos, D. S. Stable molecular transformation of *Toxoplasma gondii*: a selectable dihydrofolate reductase-thymidylate synthase marker based on drug-resistance mutations in malaria. *Proc. Natl. Acad. Sci. USA* **90**, 11703-11707 (1993).

33. Rug, M. & Maier, A.G. Transfection of *Plasmodium falciparum*. *Methods Mol. Biol.* **923**, 75-98 (2013).

34. Chambouvet, A. et al. Cryptic infection of a broad taxonomic and geographic diversity of tadpoles by Perkinsea protists. *Proc. Natl. Acad. Sci. USA* **112**, E4743-4751 (2015).

35. Barbrook, A. C., Howe, C., & Nisbet, R. Breaking up is hard to do: the complexity of the dinoflagellate chloroplast genome. *Perspect. Phycol.* https://doi.org/10.1127/pip/2018/0084 (2018).

36. Fernández Robledo, J. A., Lin, Z. & Vasta, G. R. Transfection of the protozoan parasite *Perkinsus marinus*. *Mol. Biochem. Parasitol.* **157**, 44-53 (2008).

37. Sakamoto, H. et al. Puromycin selection for stable transfectants of the oyster-infecting parasite *Perkinsus marinus*. *Parasitol. Int.* **69**, 13-16 (2018).

38. Wong, J. T. Y. & Whiteley, A. An improved method of cell cycle synchronisation for the heterotrophic dinoflagellate *Crypthecodinium cohnii* Biecheler analyzed by flow cytometry. *J. Exp. Mar. Biol. Ecol.* **197**, 91-99 (1996.).

39. Kwok, A. C., Mak, C. C., Wong, F. T. & Wong, J. T. Novel method for preparing spheroplasts from cells with an internal cellulosic cell wall. *Eukaryot. Cell* **6**, 563-567 (2007).

40. Gomaa, F., García, P. A., Delaney, J., Girguis, P. R., Buie, C. R., Edgcomb, V. P. Toward establishing model organisms for marine protists: Successful transfection protocols for *Parabodo caudatus* (Kinetoplastida: Excavata). *Env. Microbiol.* **19**, 3487-3499 (2017).

41. Nimmo, I. C. et al. Genetic transformation of the dinoflagellate chloroplast. doi: bioXRiv https://doi.org/10.1101/452144 (2018).

42. Chen, J. E., Barbrook, A. C., Cui, G., Howe, C. J. & Aranda, M. The genetic intractability of *Symbiodinium microadriaticum* to standard algal transformation methods. *PLoS ONE* **14**, e0211936 (2019).

43. Sprecher, B. N., Zhang, H. & Lin, S. Nuclear gene transformation in a dinoflagellate. *bioRxiv* 602821 (2019).

44. Zhang, H. et al. Signal recognition particle RNA in dinoflagellates and the perkinsid *Perkinsus marinus*. *Protist* **164**, 748-761 (2013).

45. Adl, S.M. et al. Revision to the classification, nomenclature and diversity of eukaryotes. *J. Euk. Microbiol.* **66**, 4-119 (2019).

46. Matthews, K.R. 25 years of African trypanosome research: From description to molecular dissection and new drug discovery. *Mol. Biochem. Parasitol*. **200**, 30-40 (2015).

47. Opperdoes, F. R., Butenko, A., Flegontov, P., Yurchenko, V. & Lukeš, J. Comparative metabolism of free-living *Bodo saltans* and parasitic trypanosomatids. *J. Eukaryot. Microbiol.* **63**, 657-678 (2016).

48. Kaur, B., et al. Transformation of *Diplonema papillatum*, the type species of the highly diverse and abundant marine micro-eukaryotes Diplonemida (Euglenozoa). *Env. Microbiol.* **20**, 1030-1040 (2018).

49. Parra-Acero, H. et al. Transfection of *Capsaspora owczarzaki*, a close unicellular relative of animals. *Development* **145**, 162107 (2018).

50. Suga, H. & Ruiz-Trillo, I. Development of ichthyosporean sheds light on the origin of metazoan multicellularity. *Dev. Biol.* **377**, 284-292 (2013).

51. Booth, D., Middleton, H. & King, N. Choanoflagellate transfection illuminates their cell biology and the ancestry of animal septins. *Mol. Biol. Cell*. **29**, 3026-38 (2018).

52. Waller, R. F. et al. Strength in numbers: collaborative science for new experimental model systems. *PLoS Biol.* **16**, e2006333 (2018)

FIGURE LEGENDS

Fig. 1. | Phylogenetic relationships and status of transfection of marine unicellular eukaryotes. A phylogenetically-informed approach was used to select protists for concerted genetic manipulation efforts. A schematic view of the eukaryotic tree of life with effigies of

main representatives based on Keeling (2019). Colour-coordinated species we have attempted to genetically modify, are listed below. Current transformability status is schematized in circles indicating: DNA delivered and shown to be expressed (yellow); DNA delivered, but no expression seen (grey); no successful transformation achieved despite efforts (blue). Delivery methods and construct types are shown pictorially. Overall, protocols and specific reagents are available to transfect 23 protist species belonging to 7 eukaryotic supergroups.

Fig. 2. | Transformation Roadmap for the creation of genetically tractable systems.

(**A**) **Vector design and construction**. Alternative routes employing a range of information and strategies are shown. (**B**) **Transformation approaches**. All methods (chemical, physical or biological) for introducing DNA/RNA/protein into a living cell are shown using icons. We highly recommend testing several of them, since successful DNA delivery depends on a number of specific features of each organism. (**C**) **Protocol**. Key features needed to obtain and demonstrate a successful transformation are listed in an abbreviated form.

Fig. 3. | Proof of successful transformation by epifluorescence.

Fluorescent microscopy images showing the transformants and wild type cells of 11 protist species. Colored boxes behind species names reflect supergroup assignments in Fig. 1. Scale bars are as follows: 10 µm for *Thalassiosira pseudonana*, *Amorphochlora* (*Lotharella*) *amoebiformis*, *Bodo saltans*, *Naegleria gruberi*, *Abeoforma whisleri*, and *Salpingoeca rosetta*; 11 µm for *Crypthecodinium cohnii*; 15 µm for *Perkinsus marinus*; 20 µm for *Fragilariopsis cylindrus* and *Oxyrrhis marina*; 100 µm for *Pseudo-nitzschia multiseries.*

Fig. 4. | Various proofs of successful transformation.

FACS and other methods were used to confirm transformation in two prasinophytes (**A, B**), one haptophyte (**C**), one stramenopile (**D**), two dinoflagellates (**E, F**) and one diplonemid (**G**). (**A**) *In vivo* luminescence of 14 *B. prasinos* transformants resistant to G418 depicted as relative luminescence unit (RLU) per 5 s and a corresponding gel showing PCR amplification from DNA of transformants of pH4:KanMx (primers 1 and 2) and pHAPT: luciferase sequences (primers 3 and 4). (**B**) FACS analysis of *M. commoda* cells in two treatments: controls (wild type [WT] or "no-pulse"), in which constructs were added but no electroporation pulse applied, and in the treatment to which a pulse was applied. Note that lower panels include only the population of healthy cells selected using the depicted gate in upper panels. Bar graphs show the mean and standard deviation of eGFP fluorescence from biological triplicates in the same experiment, analyzed as control (WT or "non-pulse") and pulsed (EW-113 treatment, with cells in the latter treatment analyzed as non-transformed, all eGFP and high GFP (cells for which eGFP fluorescence was an order of magnitude higher than in controls). Transformation efficiencies also reflect mean and standard deviations of biological triplicates. (**C**) Expression of NAT in pIgNAT transformed *I. galbana*. RT-PCR products from transformed cells resistant to nourseothricin. (**D**) FACS analysis of *N. oceanica* control cells (no plasmid added but pulse applied) and cells subjected to a pulse with a plasmid, after which a subset of cells appeared to have been transformed at 24 h. Product size (arrow) is 180 bp. (**E**) Transformation of *A. carterae* chloroplast genome with pAmpChl. RT-PCR with or without reverse transcriptase (RT), as indicated. Size of band (arrow) is 560 bp. (**F**) RT-PCR of the Neo gene in *Karlodinium* transformant "N6" under selection with kanamycin and wild type cells that were not grown under antibiotic selection. "-" and "+" depict negative (no template) and positive (neo gene as template) PCR controls, respectively. "RNA –" depicts no reverse transcriptase control, which gave negative results, and "-N" depicts nested PCR negative control. cDNA libraries were made with 200 ng of RNA from wild type and CA-137 N6 cells. (**G**) Western blot of *D.*

papillatum wild type (WT) and C4 and C5 transformants that express the V5-tagged aminoglycoside 3'-phosphotransferase (Neo). Monoclonal mouse α-V5 antibodies (1:2,000) and secondary α-mouse antibodies coupled to horseradish peroxidase (1:1,000) were used for visualisation. V5 tagged-mNeonGreen cell line of *T. brucei* cells served as a positive control and mouse anti-α-tubulin antibodies (1:5,000) were used as a loading control.

Table 1: Parameters used for successful transformation of species shown in Fig. 3 and 4.

Species	Transformation Method/ Device	Cell number	Vector;Amount (µg)	Promotor	Regulatory elements	Drug selection (µg/ml)	Time selection (Day)	Efficiency (%)	Status (Stable/ Transient)	Reporter	Evidence transformation	protocols.io link
Archaeoplastids												
Ostreococcus lucimarinus	Electroporation Genepulser II	1-2x10^9	Plasmid PotLuc; Linear; 5	HAPT, Histone H4 *O. tauri*	None	G418 (1000)	10-21	<0.0001	S	Luc	G418 resist, Luminescence	Link Link Link
Bathycoccus prasinos	Electroporation Genepulser II	1-2x10^9	Fusion PCR *p*HAPT: *p*LucpH4:KanMx Linear; 5	HAPT, Histone H4 Endogenous	None	G418 (1000)	10-21	<0.0001	S	Luc	G418 resist, Luminescence PCR	Link Link Link
Micromonas commoda	Electroporation Lonza-Nucleofector	3 x 10^7	RPS9pro^{Mco}-eGFP-NLS-RPS9ter in pUC05-AMP; Circular; 10-20	Endogenous, ribosomal protein S9;	Endogenous, ribosomal protein S9;	n/a	2-6	5.6±1.3	T*	eGFP	Per cell eGFP Fluorescence	Pending
	Electroporation Lonza-Nucleofector	3 x 10^7	H3pro^{Mpo}-LUC; Circular; 10-20	Histone H3 5' UTR from *M. polaris*	Histone H3 3' end formation - histone stem loop from *M. polaris*	n/a	3	n/a (Luc. assay is bulk, not per cell)	T*	NanoLuc®	Luminescence	Pending
Tetraselmis striata	Biorad Biolistics PDS-1000/He biolistics system	2.0x10^7	pACTpro:Ble; Linear; 1.0	Actin, *T. striata*	Actin, *T. striata*	Zeocin (150)	21-28		S		Zeocin resist, PCR	Link
Haptophytes												
Isochrysis galbana	Biolistics PDS-1000/He	1-2x10^6	pIgNAT; Circular; 1	Hsp70 *E. huxleyi*	Heterologous	Nourseothricin (80-150)	14	<0.0001	S	None	Nourseothricin resistance, PCR, RT-PCR	Link Link
Rhizarians												
Amorphochlora (Lotharella) amoebiformis	Electroporation Gene Pulser Xcell	0.5-1×10^7	GFP-Rubisco; Circular; 30-50	rbcS1, Endogenous	rbcS1 Endogenous	*Manual selection of fluorescent cells	n/a	n/a	S/T	GFP	Fluorescence	Link
Stramenopiles												
Fragilariopsis cylindrus	Biorad Biolistics PDS-1000/He biolistics system	5x10^7	pUC:FCP:ShBle:FCP:eGFP; Circular; 1	FCP, Endogenous	None	Zeocin (100)	21 – 49	0.00003 (30 cfu/10^8 cells)	S	eGFP	Zeocin resist, Fluorescence, PCR	Link Link
Thalassiosira pseudonana	Bacterial conjugation	4x10^7	TpSll3p-eGFP in pTpPuc3; Circular; n/a	Endogenous	Endogenous	Nourseothricin (100 in plates, 200 in liquid culture)	~14	~10	T	eGFP	Nourseothricin resistance, colony PCR, fluorescence	Link
Pseudo-nitzschia multiseries	Conjugation	1x10^5	Pm_actP_egfp_actT; pPtPUC3	Pm actin; Pt fcpB,	None, other than contained in Promoter/ter	Manual selection,of fluorescent cells in LGTA;	24h, 7	<0.1%	T	eGFP, shble	Fluorescence, vector targeted PCR on gDNA	Link

					m	zeocin [200],						
Aurantiochytrium limacinum	Bio – Rad Gene Pulser (165-2076)	1×10^{8}	18GZG plasmid; Linear; 1-10	Endogenous GAPDH	None	Zeocin (100)	5-7	44 per µg of DNA	S	GFP	Zeocin resist., PCR, Southern, Fluorescence	Link
Nannochloropsis oceanica	Electroporation Genepulser II	$1x10^{9}$	pMOD, Linear/Circular; ,0.1-1	CMV	None	None	0.1-1	20 (linear) 1-2 (circular)	T	mTagBFP2	Fluorescence	Link
Phaeodactylum tricornutum	Bacterial-conjugation	$4x10^{7}$	hCas9-2A-shble PtpBR episome 100uL E.coli OD_{600}=0.9	FcpF-hCas9 psRNA-sgRNA	Cen6-Arsh4-His3 centromere	Phleomycin (50) Zeocin (100)	10-16	$1.25e^{-5}$ ~500 cfu	S	shble (Cas9) yfp VENUS	Phleoycin resistance, PCR maintained episome, PCR Cas9 target site	Link
Alveolates												
Perkinsus marinus	Electroporation LONZA-Nucleofector Glass beads abrasion (425-600 µm)	$5\text{-}7x10^{7}$	*p*PmMOE-GFP; Linear-Circular (1:1); 5	Endogenous	Endogenous	FACS Blasticidin(50-200) Pur (10-50) Ble (50-200)	Drug: 20-60 FACS: 3	0.01-5	S	GFP, mCherry	Fluorescence Sequencing	Link Link Link
Oxyrrhis marina	Electroporation Gene Pulser Xcell; Chemical ($CaCl_2$)	$1\text{-}5\times10^{6}$ $1x10^{5}$	Fluorescently labelled DNA (5-25 µg) or FITC-dextran; mCherry	n/a Endogenous hsp90	n/a Endogenous hsp90	n/a	n/a	0.5-5%	T	mCherry	Fluorescence	Link Link Link Link
Karlodinium veneficum	Electroporation	$4x10^{5}$	linear-DinoIII-neo; Linear; 2	Endogenous	Endogenous	Kan (150)	7	0.0005	S (3 mon)	n/a	RT-PCR	Link
Crypthecodinium cohnii	Electroporation LONZA-Nucleofector		Stained DNA (739 bp); Linear; 1	None	None	n/a	n/a	<0.001	T	Fluorescence	Fluorescence	Link
Amphidinium carterae (chloroplast)	Biorad Biolistics PDS-1000/He biolistics system	$2.5x10^{7}$	*p*AmpChl; Circular; 0.5	Endogenous	Endogenous	CAF (20)	3 onwards	n/a	S	Ab res	RT-PCR Phenotype	Link
Discobans (Euglenozoans and Heteroloboseans)												
Bodo saltans	Electroporation Nepa21	$1\text{-}1.5x10^{7}$	Bs-EF1- a C-terminal tagging; Linear; 3-5	Endogenous	Endogenous	G418 (3)	7-9		S	GFP	Fluorescence	Link
Diplonema papillatum	Electroporation LONZA-Nucleofector	$5x10^{7}$	*p*57-V5+Neo^{R}; Linear; 3	Endogenous	Endogenous	G418 (75)	7-14	~5.5	S	n/a	Western blot (resistance marker)	Link
Naegleria gruberi	Electroporation BioRad Gene Pulser xCell	$5x10^{6}$	*p*NAEG-HYG; Circular; 4	Endogenous	Endogenous	G418 (300) Neo (700)	15-28	80	T	GFP	Western blot (resistance marker)	Link

											Fluorescence	
Opisthokonts												
Abeoforma whisleri	Electroporation LONZA-Nucleofector	$3x10^5$	Awhis_H2Bvenus + *p*UC19; Circular; 1-5+ 40 carrier	Endogenous	Endogenous	n/a	10-15	1	T	Venus	Fluorescence	Link
Salpingoeca rosetta	Electroporation LONZA-Nucleofector	$4x10^5$	SrActmCherry-CCTLL + *p*UC19; Circular; 1-10 + 40 carrier	Endogenous	Endogenous	Pur (80)	10-12		S	mCherry	Gene Expression (Luc, Fluorescence) / resistance	Link

*may be stable but overgrown by wild-type strain

Abbreviations: n/a, not applicable; NLS, Nuclear Localization Signal;

1

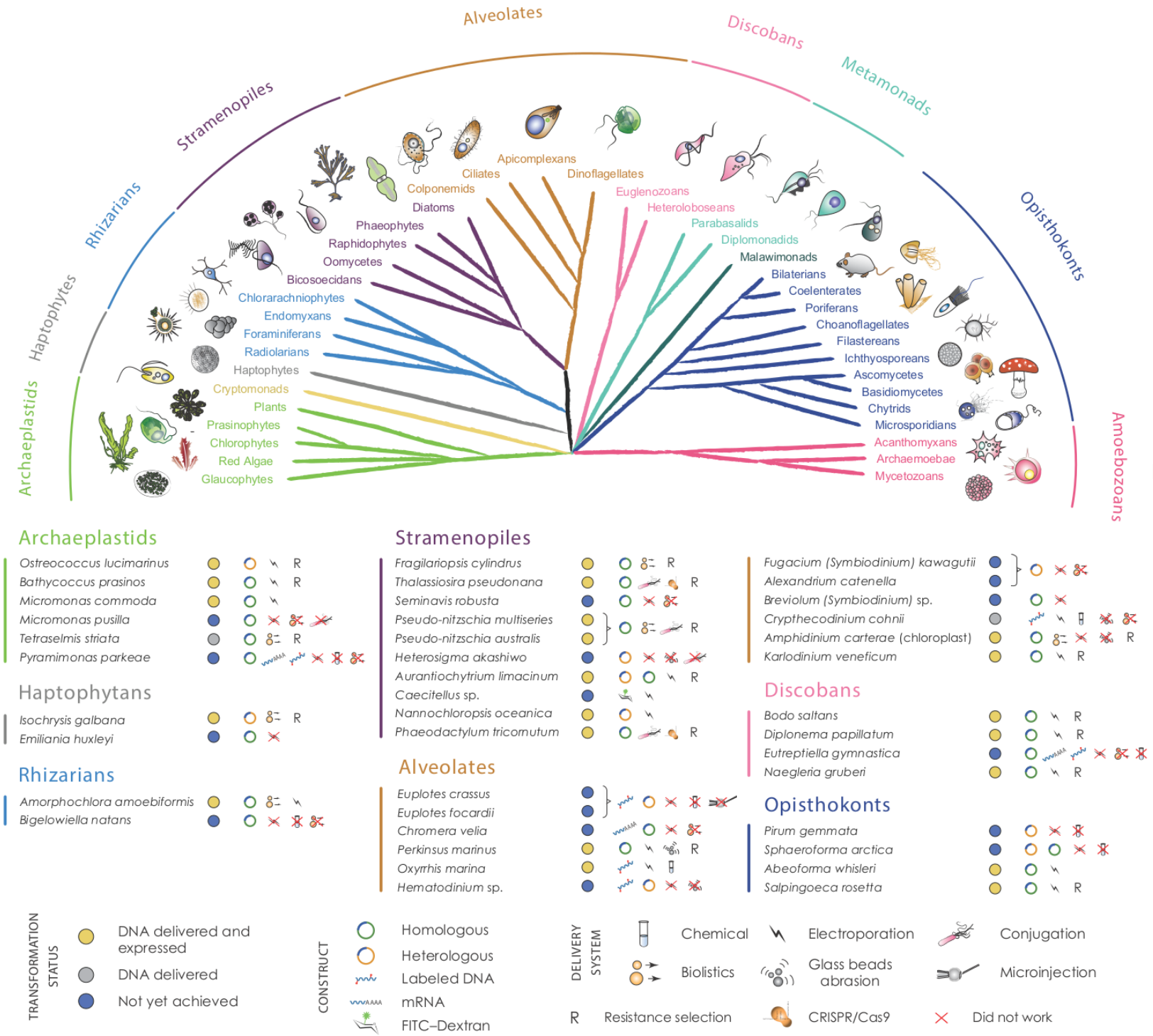
Alveolates
Discobans
Metamonads
Stramenopiles
Rhizarians
Haptophytes
Archaeplastids
Opisthokonts
Amoebozoans
Apicomplexans
Ciliates
Dinoflagellates
Colponemids
Euglenozoans
Diatoms
Heteroloboseans
Phaeophytes
Parabasalids
Raphidophytes
Diplomonadids
Oomycetes
Malawimonads
Bicosoecidans
Bilaterians
Chlorarachniophytes
Coelenterates
Endomyxans
Poriferans
Foraminiferans
Choanoflagellates
Radiolarians
Filastereans
Haptophytes
Ichthyosporeans
Cryptomonads
Ascomycetes
Plants
Basidiomycetes
Prasinophytes
Chytrids
Chlorophytes
Microsporidians
Red Algae
Acanthomyxans
Glaucophytes
Archaemoebae
Mycetozoans
Archaeplastids
Ostreococcus lucimarinus
Bathycoccus prasinos
Micromonas commoda
Micromonas pusilla
Tetraselmis striata
Pyramimonas parkeae
Haptophytans
Isochrysis galbana
Emiliania huxleyi
Rhizarians
Amorphochlora amoebiformis
Bigelowiella natans
Stramenopiles
Fragilariopsis cylindrus
Thalassiosira pseudonana
Seminavis robusta
Pseudo-nitzschia multiseries
Pseudo-nitzschia australis
Heterosigma akashiwo
Aurantiochytrium limacinum
Caecitellus sp.
Nannochloropsis oceanica
Phaeodactylum tricornutum
Alveolates
Euplotes crassus
Euplotes focardii
Chromera velia
Perkinsus marinus
Oxyrrhis marina
Hematodinium sp.
Fugacium (Symbiodinium) kawagutii
Alexandrium catenella
Breviolum (Symbiodinium) sp.
Crypthecodinium cohnii
Amphidinium carterae (chloroplast)
Karlodinium veneficum
Discobans
Bodo saltans
Diplonema papillatum
Eutreptiella gymnastica
Naegleria gruberi
Opisthokonts
Pirum gemmata
Sphaeroforma arctica
Abeoforma whisleri
Salpingoeca rosetta
R
TRANSFORMATION STATUS
DNA delivered and expressed
DNA delivered
Not yet achieved
CONSTRUCT
Homologous
Heterologous
Labeled DNA
mRNA
FITC–Dextran
DELIVERY SYSTEM
Chemical
Electroporation
Conjugation
Biolistics
Glass beads abrasion
Microinjection
R Resistance selection
CRISPR/Cas9
Did not work

2

a

Vector construction

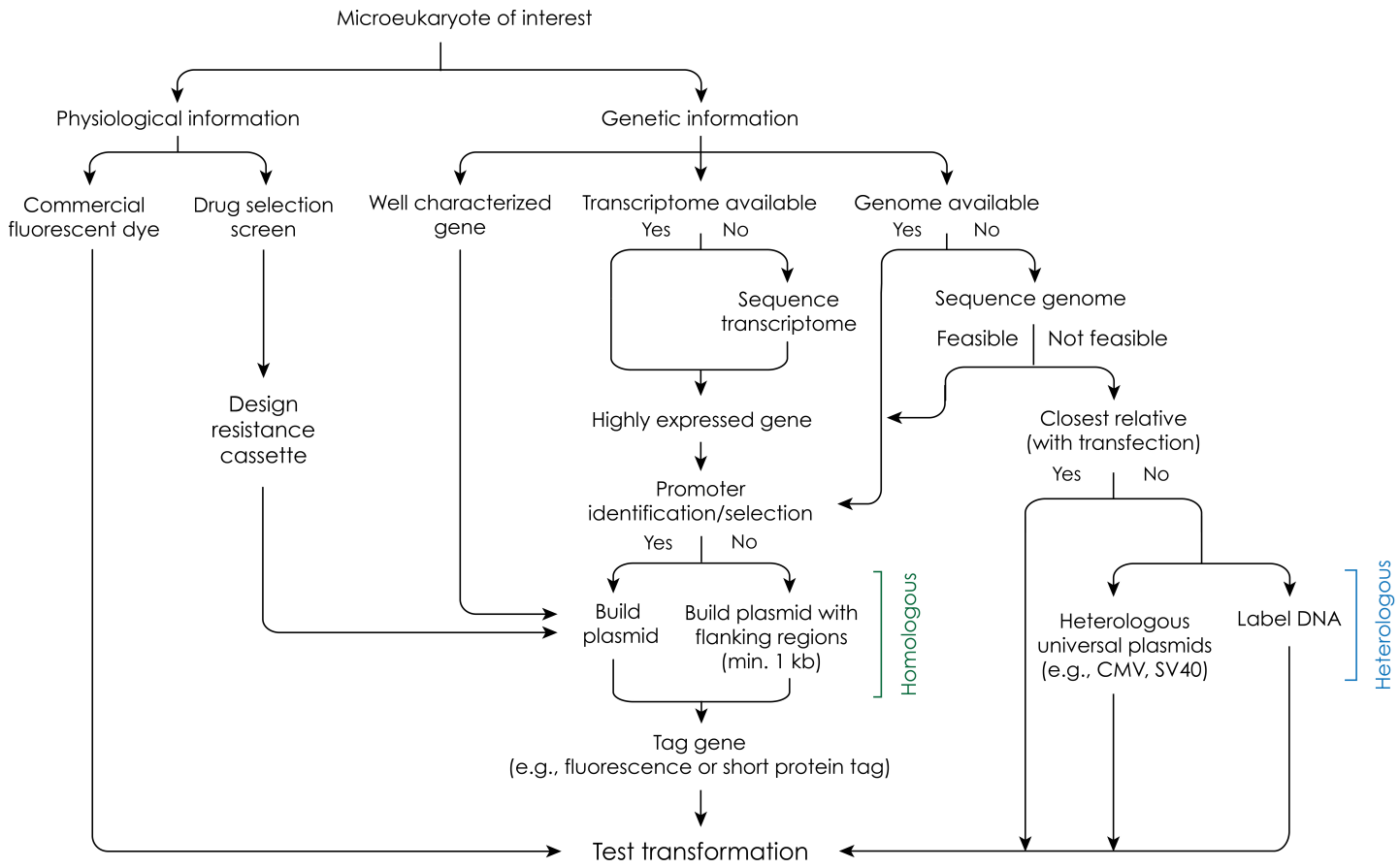

b

Transformation approaches

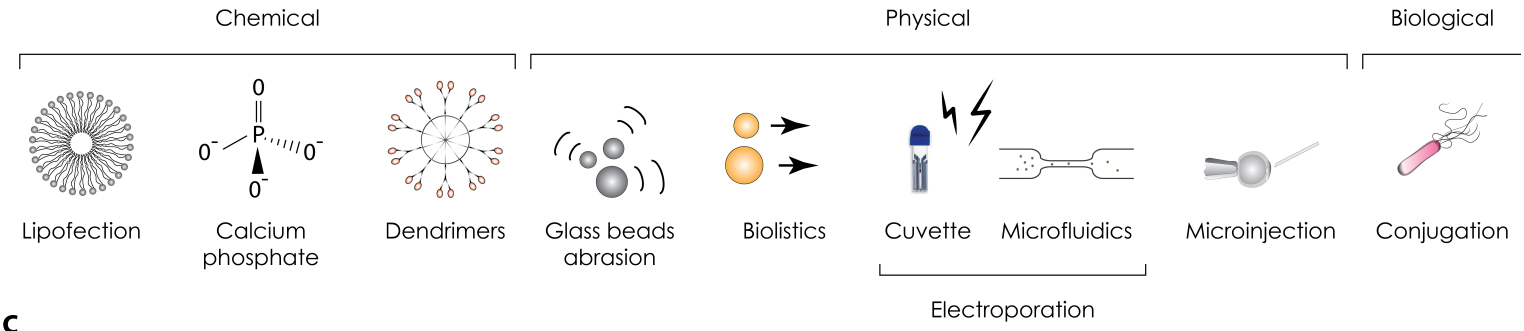

c

Protocol

Organism

- Description (life cycle stages)
- Strain
- Growth conditions and media
- Maximum cell density
- Autofluorescence
- Genome/transcriptome availability
- Cryopreservation

Resistance markers

- Antibiotics tested
- Assay used
- Resistance/sensitivity (IC_{50})

Constructs

- Construct name
- Origin
- Annotation
  - Promoter
  - UTRs
  - Flanking regions
  - Resistance
- Nature
  - Autonomously replicating
  - Integrative
  - Transiently

Transformation

- Method
- Parameters
  - Buffer composition
  - Program
- Cell stage and density
- DNA concentration
- Drug selection
  - Concentration
  - Time
- Efficiency

Transformants

- Clones examined
- Proof of nucleic acid uptake
  - Isolation of total DNA
  - PCR verification
  - Southern blot
- Plasmid maintenance
  - Chromosomal integration
  - Episomal
- Transcription
  - RT-PCR
  - Northern blot
- Translation
  - Western blot
  - Epifluorescence microscopy
  - Protein localization
- Phenotype
  - Growth curve
  - Description

3

Wild-type
Transformed cells
Bright field
Fluorescence
Bright field
Fluorescence
Amorphochlora amoebiformis
Fragilariopsis cylindrus
Thalassiosira pseudonana
Pseudo -nitzschia multiseries
Aurantiochytrium limacinum
Perkinsus marinus
Wild-type
Transformed cells
Bright field
Fluorescence
Bright field
Fluorescence
Oxyrrhis marina
Crypthecodinium cohnii
Bodo saltans
Naegleria gruberi
Abeoforma whisleri
Salpingoeca rosetta

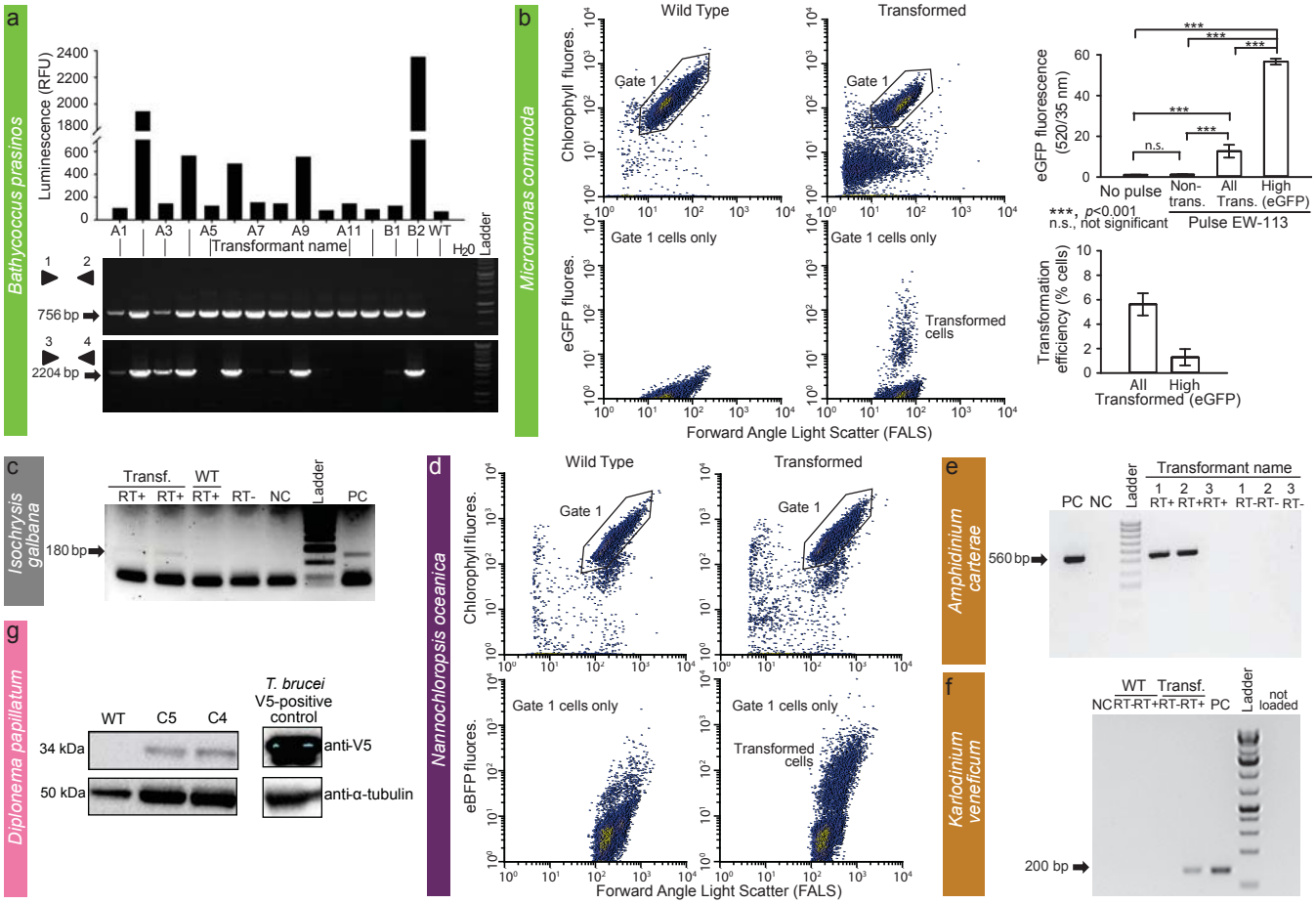
a
Bathycoccus prasinos
Luminescence (RFU)
2400
2200
2000
1800
600
400
200
0
A1
A3
A5
A7
A9
A11
B1
B2
WT
Transformant name
H2O
Ladder
1
2
756 bp
3
4
2204 bp
b
Micromonas commoda
Wild Type
Transformed
Chlorophyll fluores.
Gate 1
Gate 1 cells only
eGFP fluores.
Transformed cells
Forward Angle Light Scatter (FALS)
eGFP fluorescence (520/35 nm)
No pulse
Non-trans.
All Trans.
High (eGFP)
Pulse EW-113
***, p<0.001
n.s., not significant
Transformation efficiency (% cells)
All Transformed
High (eGFP)
c
Isochrysis galbana
Transf.
WT
RT+
RT+
RT+
RT-
NC
Ladder
PC
180 bp
g
Diplonema papillatum
WT
C5
C4
T. brucei V5-positive control
34 kDa
50 kDa
anti-V5
anti-α-tubulin
d
Nannochloropsis oceanica
Wild Type
Transformed
Chlorophyll fluores.
Gate 1
Gate 1 cells only
eBFP fluores.
Transformed cells
Forward Angle Light Scatter (FALS)
e
Amphidinium carterae
PC
NC
Ladder
Transformant name
1 RT+
2 RT+
3 RT+
1 RT-
2 RT-
3 RT-
560 bp
f
Karlodinium veneficum
WT
Transf.
NC
RT-
RT+
RT-
RT+
PC
Ladder
not loaded
200 bp